ACS Catalysis

Research Article

pubs.acs.org/acscatalysis

Investigating the Impact of Multi-Heme Pyrroloquinoline Quinone-Aldehyde Dehydrogenase Orientation on Direct Bioelectrocatalysis via Site Specific Enzyme Immobilization

Shuai Xu and Shelley D. Minteer*

Department of Chemistry, University of Utah, 315 South 1400 East, Room 2020, Salt Lake City, Utah 84112, United States

Supporting Information

ABSTRACT: To investigate the effect of the orientation of large and complex multi-subunit enzymes (MW > 50 kDa) on direct bioelectrocatalysis, we immobilized enzymes known to be capable of direct electron transfer (DET) via a site specific immobilization technique to form a monolayer of biocatalysts with a uniform orientation toward the gold electrode. Six recombinant pyrroloquinoline quinone-dependent aldehyde dehydrogenases (PQQ-AlDHs) were employed, where the enzymes had been labeled with six-histidine tags (His-tag) at the N- or C-terminus of each of the three subunits. His-tags were utilized as linking sites to perform site specific immobilization of PQQ-AlDHs. Results show that the orientation of multi-subunit enzymes can affect DET greatly by varying the electron tunneling distances. The favorable orientation allowing for a minimal heme *c* electron transfer distance showed a DET rate 6.6-fold higher than that with the orientation closest to the active site of the enzyme, while the unfavorable attachment to a nonelectroactive subunit showed no DET.

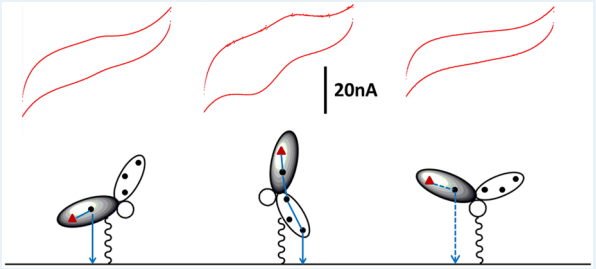

KEYWORDS: *quinohemoproteins, PQQ-dependent dehydrogenases, direct electron transfer, bioelectrocatalysis, enzyme orientation*

INTRODUCTION

Using enzymes as biocatalysts in fuel cells not only has expanded the diversity of the potential fuels and offered the opportunity to utilize more complex fuel molecules (i.e., sugars,[1] fatty acids,[2] and alcohols[3]) as energy sources but also has allowed engineering of enzymes to be promiscuous and utilize a variety of substrates[4] as well as allowed for deeper oxidation of complex fuels via enzyme cascades.[3,5] There are two methods of coupling an enzymatic reaction to an electrode. The first mechanism discovered was based on using a redox mediator to transfer the electrons from the active site of the enzyme to the electrode surface, which is commonly called mediated electron transfer (MET). Early mediated electron transfer systems involved small molecule diffusional mediators. In this case, the mediators participated directly in the catalytic reaction by reacting directly with the enzyme or its cofactor to become oxidized or reduced and diffuse to the electrode surface, where the rapid regeneration of the mediators takes place. In the past two decades, many immobilized mediators have been used.[6] This electron transfer (ET) mechanism requires certain characteristics of the mediator. (1) The mediators have to be stable at multiple oxidation states. (2) The regeneration reaction at the electrode surface has to be reversible. (3) Those mediators have to have long lifetimes themselves.[7] Those requirements have been challenging for the practical or commercial utilization of mediators in enzymatic biofuel cells. The other electron transfer method is a "mediatorless" process or direct electron transfer (DET).[8] In this process, the enzymes act as "electron transducers" and directly convert the chemical signal to an electrical one through internal charge transfer. Using enzymes that are capable of facile DET eliminates the need for mediator molecules that can be non-selective, decrease stability, and decrease the open circuit potential of the biofuel cell, which limit the optimal performance of the biofuel cell. The first studies of DET enzymes involved examining enzymes such as laccase that showed the ability to catalyze the four-electron reduction of O_2 to H_2O through direct electron transfer from the electrode surface to the active site. More recently, O_2 reduction at a more neutral pH was observed with the DET-capable enzyme bilirubin oxidase (BOD).[9] These enzymes are both multicopper oxidases, and to date, a variety of multicopper oxidases have shown facile direct electron transfer for use in the cathode compartment of enzymatic biofuel cells. Anodic direct bioelectrocatalysis has been more rare. Although enzymes capable of catalyzing oxidation at the anodic compartment of biofuel cells have also been shown to demonstrate DET, many anodic enzymes are NAD-dependent and therefore are not capable of direct electron transfer. Many of the enzymes that have been shown to perform direct bioelectrocatalysis contain redox active metal centers that perform the intrinsic transfer of electrons. For example, the heme group of several enzymes is

Received: April 25, 2013
Revised: June 14, 2013
Published: June 28, 2013

   dx.doi.org/10.1021/cs400316b | ACS Catal. 2013, 3, 1756−1763

capable of existing in several redox state and transfer resultant electrons produced at the active site of the enzyme. One of the prime examples of this has been cellobiose dehydrogenase, which contains a FAD cofactor and a heme center and is capable of direct electron transfer.[10] Another class of heme-containing enzymes that can undergo direct bioelectrocatalysis consists of quinohemoproteins.

Pyrroloquinoline quinone (PQQ)-dependent enzymes have shown to be able to catalyze the oxidation of substrates like alcohol, aldehyde, and sugars.[11] These quinohemoproteins contain multi-heme groups in different subunits, and electrons can be transferred through single-heme or multi-heme pathways before they arrive at the surface of the electrode.[12] PQQ-dependent enzymes are generally divided into three types: (1) non-heme PQQ-dependent enzymes such as PQQ-glucose dehydrogenase, (2) single-heme PQQ-dependent enzymes such as PQQ-dependent sorbitol dehydrogenase,[13] and (3) multi-heme PQQ-dependent enzymes. The most well-known are PQQ-dependent alcohol and aldehyde dehydrogenases. DET was reported to be achieved most frequently with these multi-heme biocatalysts, and electron transfer was demonstrated to occur through a single heme or multi-heme pathway.[14]

However, the conditions of DET for complex multi-subunit proteins are closely related to the proximity and orientation of the enzymes toward the electrode surface for electron tunneling to occur,[8] allowing the biocatalytic reaction to be the limiting process. In the case of quinohemoproteins, the closest heme group in the enzyme to the electrode surface needs to be within electron tunneling distance. For larger proteins, the orientation of the enzyme toward the electrode surface will not only affect the proximity of the redox active site and the electrode surface but also determine whether the substrate active site is accessible or blocked by the electrode. In the past few years, different methods have been employed to increase the proximity. Conductive polymers,[14b] carbon nanotubes (CNTs),[15] and sol−gel/carbon nanotube composite electrodes[16] have been utilized to increase the electrode surface area and roughness, thus decreasing the distance between the redox active site and the electrode surface. However, all of these techniques decrease the electron transfer distance with an anisotropic enzyme orientation, and contributions to electron transfer from differently oriented proteins were not discussed.

Approaches for isotropic alignment of the DET enzyme on the electrode surface were reported with major methods, including (a) the reconstitute apoenzyme on the preimmobilized cofactor to yield a DET favorable orientation[17]and (b) binding of enzyme molecules through a unique functional group,[18] but most lack in their discussion of electron transfer properties or comparison of electron transfer from different orientations of the same protein.[19] In this paper, we address how the orientation of these multi-subunit, multi-heme enzymes toward the electrode surface will affect the electron transfer rate and thus influence the bioelectrochemical performance, by aligning PQQ-AlDH on the electrode surface through the six-histidine tag (His-tag) functional group. As mentioned above, PQQ-dependent enzymes have been shown to be capable of DET, because of the existence of multiple heme *c* groups that act as DET charge carriers. In this study, we have chosen PQQ-dependent aldehyde dehydrogenase (PQQ-AlDH) from *Gluconobacter* sp. to demonstrate the importance of enzyme orientation. PQQ-AlDH consists of three subunits: one subunit that contains cofactor PQQ and one heme *c* (subunit I), one subunit that contains three heme *c* moieties (subunit II), and one small subunit that is a peptide that bridges the two larger subunits together and maintains the integrity of the whole protein structure but does not contain any electroactive species (subunit III). Genetically modified PQQ-AlDHs with a His-tag at the N- or C-terminus of each subunit were used for different types of orientation specific immobilization.

To control the orientation of the enzyme, we utilized a reported method that was inspired by metal ion affinity chromatography.[20] The flat gold electrode surface was modified by attaching a nitrilotriacetic (NTA) moiety to the metal surface via a sulfhydryl group. After Ni^{2+} had been incorporated at the other end, a recombinant protein engineered to have six consecutive histidine residues (His-tag) at either the C- or N-terminus is attached by affinity to the Ni-NTA moiety. Thus, control of the orientation of the enzyme toward the electrode surface is established. The performances of DET bioanodes with different enzyme orientations were characterized and compared.

EXPERIMENTAL SECTION

Bioengineered *Gluconobacter* sp. Growth. Six bioengineered *Gluconobacter* sp. (DSM 3504) bacteria were provided by Modular Genetics, Inc.; each bacterium was engineered to express PQQ-AlDH with a His-tag in a different part of the multi-subunit protein. The six resulting enzymes have the His-tag on either the C- or N-terminus of one of the three subunits (i.e., His-tag on the C-terminus of subunit 1, His-tag on the N-terminus of subunit 2, etc.). Bacteria were cultivated aerobically in a basal medium containing yeast extract, D-mannitol, $(NH_4)_2HPO_4$, and $MgSO_4$ at 30 °C for 24 h, as per previous procedures for the native bacteria.[21] The cell pastes were centrifuged at 12000*g*, then washed twice in 50 mM potassium phosphate buffer, and stored at −20 °C until they were used.

Isolation of Each His-Tag PQQ-AlDH. All six His-tag PQQ-AlDHs with His-tags on different sites were isolated with the same method. Bioengineered *Gluconobacter* was thawed and suspended in 0.2 M phosphate buffer (pH 7.2) containing 1 mM $CaCl_2$, 10% sodium deoxycholate (to a final concentration of 0.5%), and 1 mL of lysozyme [10 mg of lysozyme in 1 mL of 0.3 M potassium phosphate buffer (pH 7.2)]. The solution was incubated at 4 °C while being gently stirred for 1 h followed by ultrasonication using a sonic dismembrator for 1 min at 4 °C. The solution was then centrifuged for 1 h at 12000*g* to remove insoluble materials. The crude extract was dialyzed against 0.1 M potassium phosphate buffer containing 10 mM imidazole and 10 mM mercaptoethanol overnight.

Metal ion affinity chromatography (MIAC) (Thermo Scientific) was utilized to purify target His-tag proteins with 10 mM imidazole equilibration buffer, 50 mM imidazole wash buffer, and 500 mM imidazole elution buffer. Eluates were washed with 50 mM potassium phosphate buffer to remove the imidazole residue that can interfere with the enzyme activity assay and electrode modification. The purity of the enzymes was validated with native protein gels and sodium dodecyl sulfate−polyacrylamide gel electrophoresis (SDS−PAGE) gels, as per the procedures in the Supporting Information. Representative gels are also shown in the Supporting Information.

Surface Modification of Gold Electrodes. The self assembled monolayer (SAM) electrode modification method was reported by Ataka et al.[20] Polished gold electrodes were

dx.doi.org/10.1021/cs400316b | *ACS Catal.* 2013, 3, 1756−1763

exposed to 1 mg/mL dithiodis(succinimidylpropionate) [DTSP (Fluka)] in dimethyl sulfoxide for 30 min. DTSP forms a monolayer on gold through covalent linkage to the sulfur group. The self-assembled monolayer (SAM) was then immersed in an aqueous solution of 150 mM amino-nitrilotriacetic acid [ANTA (Sigma)] in 0.5 M K_2CO_3 buffer (pH 9.8). Excess ANTA was removed with ultrapure water washing. The TSP-NTA-modified electrode was then incubated with 50 mM $NiSO_4$ (Sigma) to ligate the Ni^{2+} ion via the three carboxylates and the terminal amine of NTA. Finally, the TSP-NTA-Ni-modified electrode was incubated with 1 mg/mL His-tag PQQ-AlDH solutions for 12 h. PQQ-AlDHs attach to the Ni-NTA moiety through the coordination of the two nitrogens of the imidazole side chains of the His-tag.

Enzyme Activity Assay. The enzyme reaction mixture consists of 1.5 mL of 50 mM potassium phosphate buffer (pH 7.3), 0.2 mL of 600 μM PMS (phenazine methosulfate), 0.1 mL of 700 μM DCIP (dichlorophenolindophenol), 0.01 mL of the enzyme solution, and 0.2 mL of a 0.2 M substrate solution. For PQQ-dependent aldehyde dehydrogenase, acetaldehyde and glyceraldehyde were used as substrates. The change in absorbance during a 2 min interval for each sample is measured at 37 °C at 0 and 2 min at 600 nm on a Genesys 20 spectrophotometer. The specific activity is calculated in units per milligram, where 1 unit corresponds to converting 1 μmol of substrate per minute. The molar absorptivity (ε) of DCIP was experimentally determined to be 30.

The immobilized enzyme concentration was measured with a modified UV spectrophotometric protein assay utilizing the 280 nm characteristic protein absorbance peak on a Thermo Evolution 260 Bio instrument. Each type of recombinant PQQ-AlDH was immobilized on a 1 cm^2 TSP-Ni-NTA-modified gold electrode with the method described above and then washed off with 1 mL of 500 mM imidazole in 50 mM phosphate elution buffer. UV absorbances of the wash solutions at wavelengths of 280 and 260 nm (A_{280} and A_{260}, respectively) were measured with elution buffer used as the blank. Statistical significance was determined by the t test at 95% confidence for triplicate measurements.

Electrochemical Measurements. Cyclic voltammetry (CV) was performed on a CH Instruments 611C potentiostat. Platinum and Ag/AgCl electrodes were used as counter and reference electrodes, and all measurements were performed in 50 mM potassium phosphate buffer (pH 7.4) with 0.1 M sodium nitrate as the supporting electrolyte. Electrochemical impedance spectroscopy was measured in the same buffer solution, and this measurement was performed with a Bio-Logic 150SP potentiostat.

RESULTS AND DISCUSSION

Six types of recombinant PQQ-AlDHs, which have a His-tag on different subunits, have been expressed and purified. Two of the constructs of PQQ-AlDH have the His-tag at the C- and N-terminus of subunit I (His-IC and His-IN, respectively), which is the subunit where the enzyme active site is located along with a single heme *c*. Two of the constructs have the His-tag at the C- and N-terminus of subunit II (His-IIC and His-IIN, respectively), which contains multiple heme *c* groups. Two of the constructs have the His-tag at the C- and N-terminus of subunit III (His-IIIC and His-IIIN, respectively), which is a peptide subunit that provides structural integrity but contains no electroactive species.

The strategy of this study is schematically depicted in Figure 1. By immobilizing PQQ-AlDH with the orientation determined via the histidine tags as linking sites, we achieved uniform orientations of the enzyme toward the electrode. Different specific orientations were achieved by coupling the enzyme to the electrode via His-tags on different subunits of PQQ-AlDH. Because each specific orientation is different in terms of the electron transfer distance, comparing their electrochemical properties will demonstrate the effect of enzyme orientation on direct electron transfer rate.

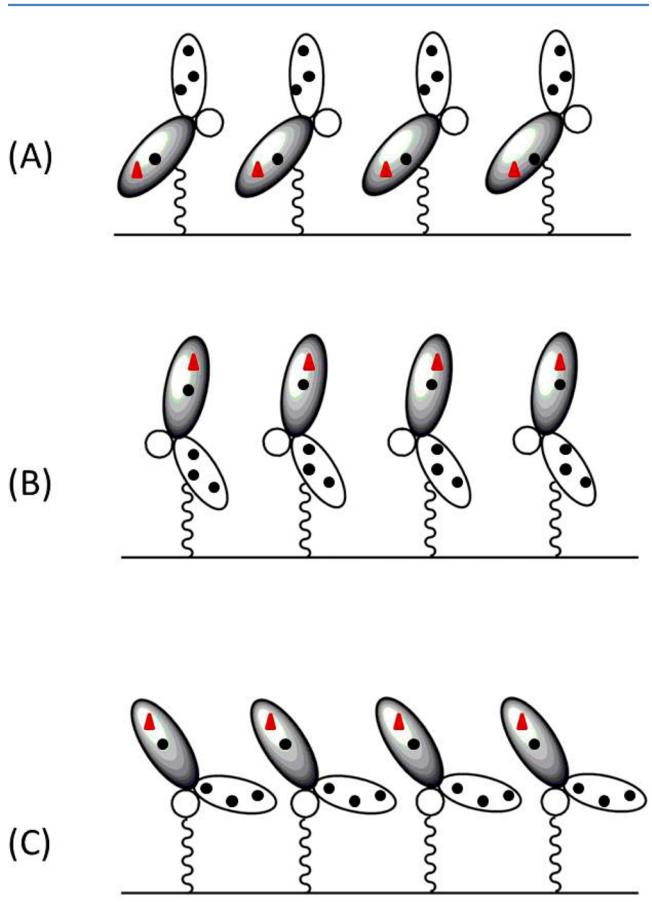

Figure 1. Schematic illustration of His-tag PQQ-AlDH with His-tag orientation controlled via immobilization on gold electrodes, where the black circles represent heme *c* groups, the red triangles represent PQQ cofactors, and the colored subunit represents the active site subunit (subunit I). (A) His-tag on subunit I as the linking site, (B) His-tag on subunit II as the linking site, and (C) His-tag on subunit III as the linking site.

His-Tag PQQ-AlDH Activity Measurements. PQQ-AlDH is a promiscuous enzyme that shows activity on a variety of different aldehydes. Six recombinant PQQ-AlDH specific activities toward two aldehydes (acetaldehyde and glyceraldehyde) were monitored throughout the purification process, as shown in Table 1. Via comparison of the specific activities before and after MIAC, results showed a roughly 10-fold purification with MIAC with all His-tag AlDHs. The purity was verified by SDS−PAGE. All AlDHs showed slightly higher activity toward glyceraldehyde than acetaldehyde. Therefore, all further electrochemical and spectroscopic measurements used glyceraldehyde as the enzyme substrate.

Gold Surface Modification. The gold surface has been modified by several steps to form a Ni-NTA-terminated self-

dx.doi.org/10.1021/cs400316b | ACS Catal. 2013, 3, 1756−1763

Table 1. Specific Activity Assay Results for Six Recombinant PQQ-AlDHs before and after Purification via Affinity Chromatography with Acetaldehyde and Glyceraldehyde as Substrates

		His-IC (units/mg)	His-IN (units/mg)	His-IIC (units/mg)	His-IIN (units/mg)	His-IIIC (units/mg)	His-IIIN (units/mg)
before MIAC	acetaldehyde	0.25 ± 0.07	0.33 ± 0.11	0.39 ± 0.12	0.25 ± 0.08	0.32 ± 0.10	0.34 ± 0.11
	glyceraldehyde	0.37 ± 0.12	0.35 ± 0.14	0.41 ± 0.18	0.31 ± 0.09	0.34 ± 0.11	0.44 ± 0.19
after MIAC	acetaldehyde	2.63 ± 0.31	2.71 ± 0.34	2.76 ± 0.25	3.40 ± 0.35	3.06 ± 0.25	3.24 ± 0.31
	glyceraldehyde	3.43 ± 0.33	4.64 ± 0.48	3.37 ± 0.39	3.65 ± 0.33	3.42 ± 0.22	3.91 ± 0.34

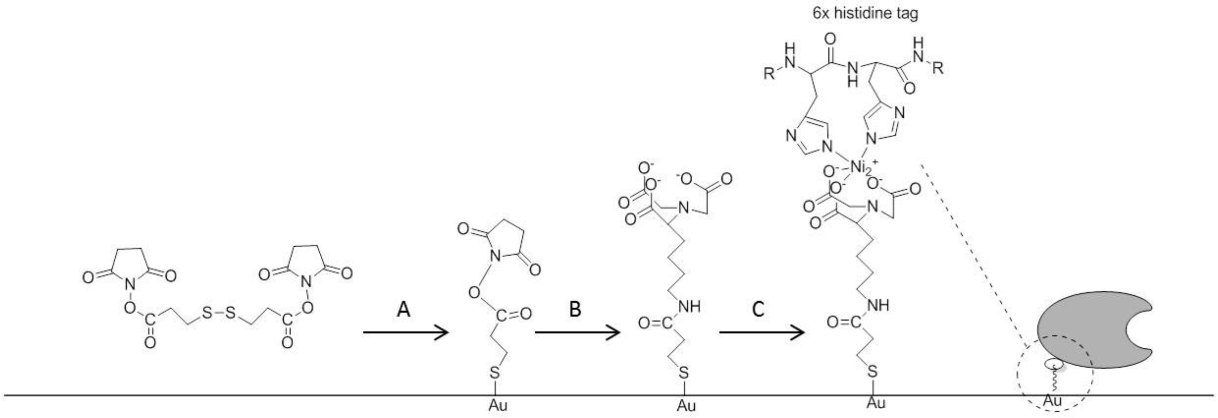

Figure 2. Gold surface modification process. (A) Self-assembly of the TSP monolayer on a flat gold electrode surface. (B) Cross-linking of ANTA with the TSP monolayer. (C) Adsorption of recombinant PQQ-AlDH on the modified electrode surface via the His-tag site.

assembled monolayer as reported previously.[20] The modification process is depicted in Figure 2. The modification process consists of three steps: (1) formation of a self-assembled monolayer of TSP on a flat gold electrode surface, followed by (2) cross-linking NTA with the TSP SAM to form a TSP-NTA layer, followed by (3) immobilization of the His-tagged enzyme on the TSP-NTA-Ni layer. To monitor the process of gold electrode modification, each SAM formation step was monitored with electrochemical impedance spectroscopy (EIS). The results are shown in Figure 3. EIS results show that, with addition of DTSP and ANTA on a gold electrode, the impedance of the electrode surface increased with the formation of the SAM, which indicated the formation of the linker monolayer. To further prove the formation of the NTA monolayer and its ability to attach to a metal ion, we have performed cyclic voltammetry with a TSP-NTA-modified gold electrode with Cu^{2+} for comparison with the previously reported immobilized Cu^{2+} oxidation potential (see the Supporting Information). A reversible peak at 0.2 V versus Ag/AgCl corresponds to the one-electron oxidation from Cu(I) to Cu(II) that matches the previously reported value.[22] This result shows that the metal ion can be successfully attached to the TSP-NTA layer.

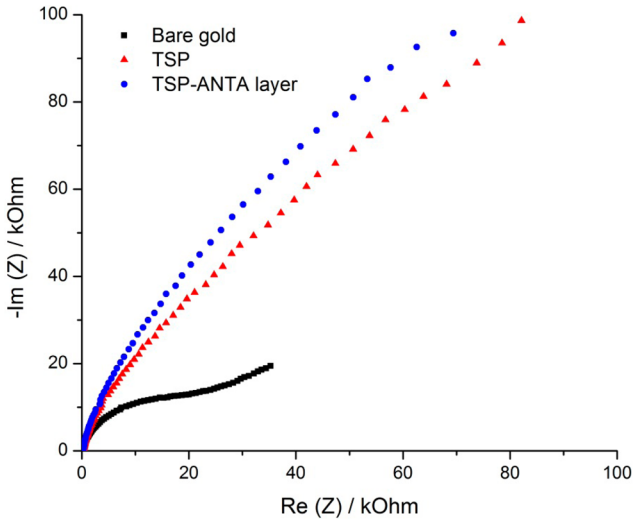

Figure 3. Electrochemical impedance spectroscopy of the formation of the immobilized layers. Measurements were taken in 50 mM phosphate buffer over a frequency range of 100 kHz to 600 mHz ($E_{applied}$ = 0.4 V vs SCE; purtubation ±5 mV).

Immobilized Enzyme Activity Measurement. To demonstrate active His-tag enzymes are successfully attached to modified electrodes, immobilized enzyme activity assays (DCIP assay described above) were performed. His-tag enzyme-loaded electrodes were exposed to assay solutions for 60 min, and absorbance changes at 600 nm were recorded. This experiment was performed for the sole purpose of demonstrating active enzymes are attached to the modified electrodes. Assay results are listed in Table 2. Glyceraldehyde was used as the enzyme substrate in the assays.

All immobilized enzyme assay results showed all immobilized recombinant PQQ-AlDHs have a statistically significant absorbance change compared to the control except for His-IIC, which indicates five active His-tag PQQ-AlDHs (His-IC, His-IN, His-IIN, His-IIIC, and His-IIIN) were successfully immobilized on modified gold electrodes. Whether His-IIC was successfully coupled with a modified gold electrode needed to be further measured with a protein concentration assay to determine the enzyme density on the electrode.

To measure the enzyme-immobilized density on the electrode for each of the six recombinant enzymes, we modified 1 cm × 1 cm gold foils as described above with six recombinant enzymes. Then, we washed off the His-tag enzymes with a 500 mM imidazole solution. After being washed, the enzymes were

dx.doi.org/10.1021/cs400316b | ACS Catal. 2013, 3, 1756−1763

Table 2. Enzyme Immobilization Densities and Specific Activities of Six Recombinant PQQ-AlDHs on Modified Gold Electrodes

	His-IC	His-IN	His-IIC	His-IIN	His-IIIC	His-IIIN	control
change in absorbance	0.056 ± 0.012	0.019 ± 0.011	0.004 ± 0.001	0.245 ± 0.035	0.192 ± 0.011	0.213 ± 0.017	0.000 ± 0.002
enzyme density (μg/cm^2)	8.5	7.0	0.7	8.5	8.5	7.0	0.7
specific activity (units/mg)	0.73 ± 0.16	0.20 ± 0.11	0.63 ± 0.16	3.21 ± 0.52	2.52 ± 0.14	2.23 ± 0.18	0.00 ± 0.32

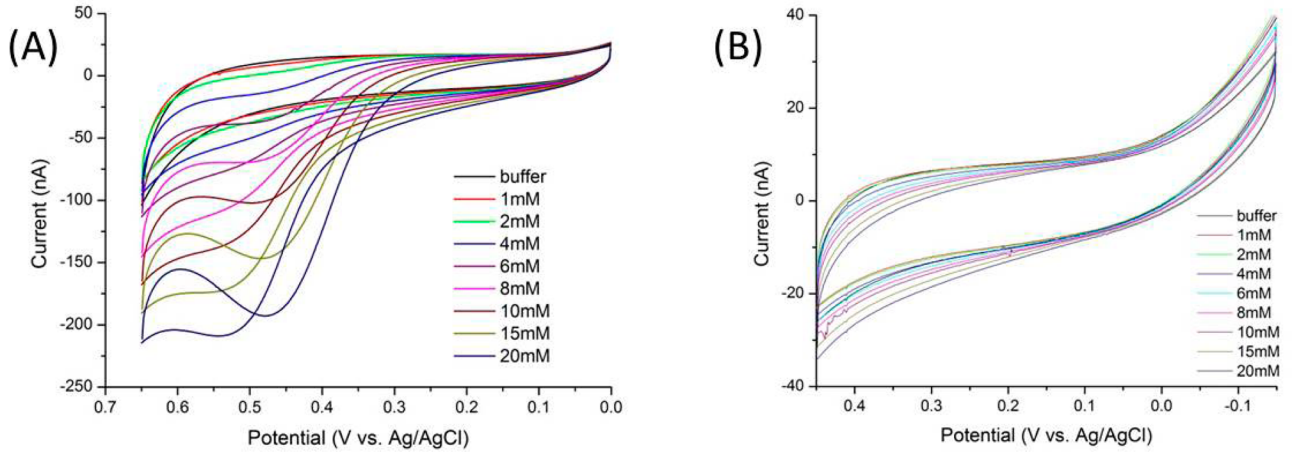

Figure 4. Cyclic voltammograms of the TSP-NTA-Ni (control)-modified gold electrode at different glyceraldehyde concentrations. The scan rate was 5 mV/s. (A) Cyclic voltammograms of control electrodes with a scan window of 0−650 mV. (B) Cyclic voltammograms of control electrodes with a scan window of −150 to 450 mV.

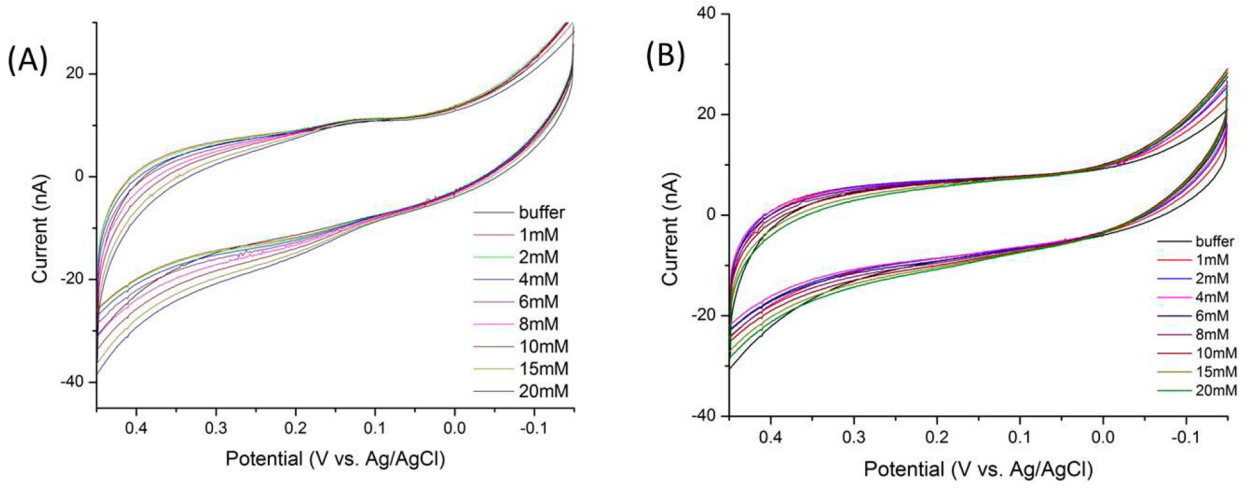

Figure 5. Cyclic voltammograms of (A) His-IC- and (B) His-IN-modified gold electrodes in a 50 mM phosphate buffer (pH 7.4) with 0.1 M KNO_3 supporting electrolyte at a scan rate of 5 mV/s. Concentrations correspond to increasing concentrations of glyceraldehyde.

rinsed with phosphate buffer to eliminate imidazole, and the protein concentrations were measured with absorbance at 280 nm and are listed in Table 2. We also performed this experiment with native PQQ-AlDH, and the results suggested no nonspecific enzyme binding to the modified electrode (see the Supporting Information).

Protein concentration assays showed that all recombinant PQQ-AlDHs attached to the modified gold electrode with a density of 7.0−8.5 μg/cm^2, except for His-IIC, which showed no significant enzyme was immobilized on the electrode. This could be that the C-terminus of subunit II cannot be sterically reached by Ni-NTA. By coupling the results of the DCIP assays and protein concentration assays, we calculated specific activities of immobilized His-tag PQQ-AlDHs. From the results, we can determine that subunit III and subunit II N-terminally tagged PQQ-AlDHs showed close to free enzyme specific activity, which means immobilization did not deactivate enzyme and the substrate is accessible to the enzyme. Subunit I-labeled PQQ-AlDH showed a lower specific activity. Enzyme activities in free solutions after purification showed similar results for all six samples, which indicates that the His-tag is not or only minimally affecting the kinetics of the enzyme. This can be explained by either a change in the substrate accessibility or minor conformational changes when enzymes are immobilized on the electrode surface. To rule out the possibility of nonspecific binding of the enzyme on the electrode, we conducted immobilized protein assays with the native enzyme, and the results showed no enzyme was bound to the modified electrode surface (same results as the blank).

dx.doi.org/10.1021/cs400316b | ACS Catal. 2013, 3, 1756−1763

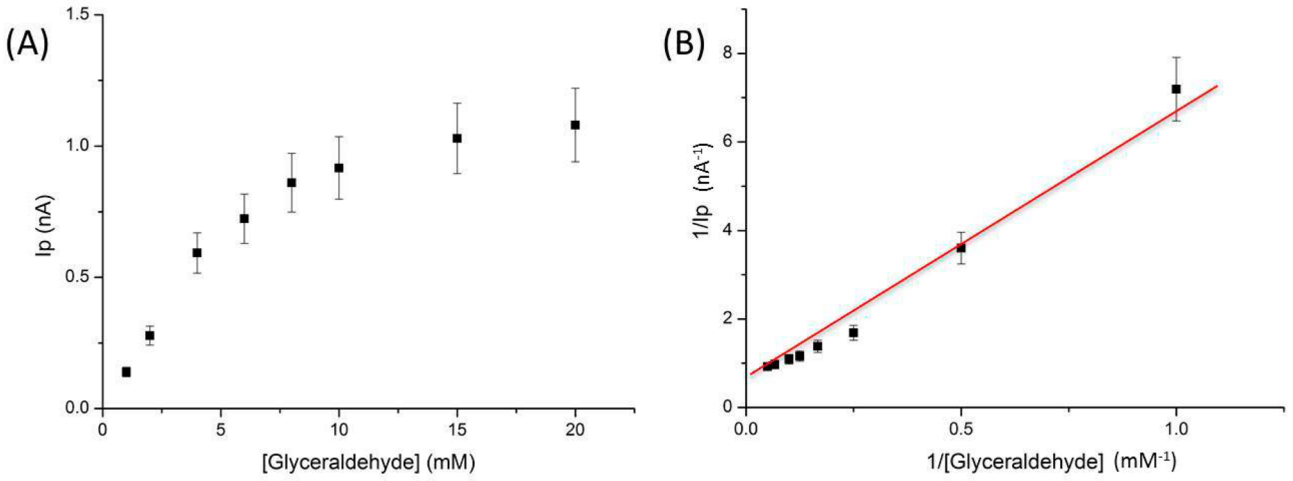

Figure 6. Calibration curve of peak current vs glyceraldehyde concentration (A) and Lineweaver–Burk plot (B) of His-IC-modified gold electrodes.

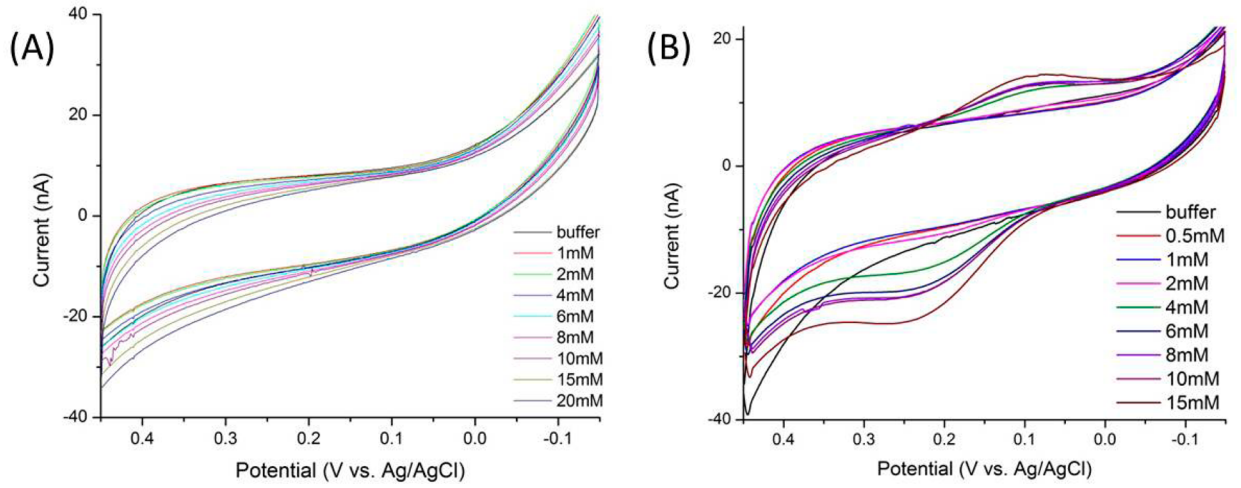

Figure 7. Cyclic voltammograms of (A) His-IIC- and (B) His-IIN-modified gold electrodes in 50 mM phosphate buffer (pH 7.4) with 0.1 M KNO_3 as the supporting electrolyte at a scan rate of 5 mV/s. Concentrations correspond to increasing concentrations of glyceraldehyde.

Electrochemical Properties of Surface-Tethered PQQ-AlDHs. Finally, the ability of the enzyme to conduct direct electron transfer (DET) was investigated with different orientations of PQQ-AlDHs. Electron transfer was probed by CV. CV was conducted with the glyceraldehyde substrate at various concentrations. TSP-NTA-Ni-modified gold electrodes without enzyme loading were used as the control.

Cyclic voltammograms of linker-modified electrodes (control electrodes without enzymes) with a wider scan window showed an oxidation peak at around 500 mV versus Ag|AgCl (Figure 4A). This peak was identified as the oxidation peak of the Ni ion catalyzing the oxidation of glyceraldehyde. PQQ-dependent aldehyde dehydrogenase should have an oxidation peak at ~190 mV versus Ag|AgCl, because the electron transfer is believed to occur through one of the heme *c* groups in subunit II, which has a potential of 190 mV versus Ag|AgCl.[23] A smaller window scan was performed on the control electrodes, and no peak was observed in the range of −150 to 450 mV (Figure 4B). Therefore, all studies of enzyme-modified electrodes used this scan window. To rule out the possibility of nonspecific binding of the enzyme on the electrode, we tested the electrochemistry of the electrodes with the native enzyme. Cyclic voltammograms showed no catalytic peak in the scan range, as shown in the Supporting Information.

After His-tag enzymes had been tethered to the modified electrode surface, electrodes were tested at different glyceraldehyde substrate solution concentrations. Cyclic voltammograms of His-IC and His-IN are shown in Figure 5. Electrons can be transferred either via the single heme *c* group in subunit I and then directly to the electrode surface or through the multiple heme *c* groups in subunit II before being released by the protein to the electrode. With subunit I-tagged PQQ-AlDH, electrons transferring to the gold electrode surface via the single heme *c* group in subunit I is a reasonable prediction. Cyclic voltammograms of His-IC showed a small catalytic peak at 203 ± 4 mV versus Ag/AgCl, while His-IN showed no peak in this scan window. The electrochemical measurements indicate that even though the two His-tags are on the same subunit, the N- and C-termini yield different orientations of the enzyme toward the electrode that result in different heme–electrode distances. The N-terminal His-tag is far from the heme *c* group in subunit I, which yields a longer space between the heme *c* and the gold electrode surface. Plots of peak current versus concentration and the Lineweaver–Burk curve of His-IC-modified electrodes are shown in Figure 6. The calibration curve of His-IC follows

dx.doi.org/10.1021/cs400316b | *ACS Catal.* 2013, 3, 1756–1763

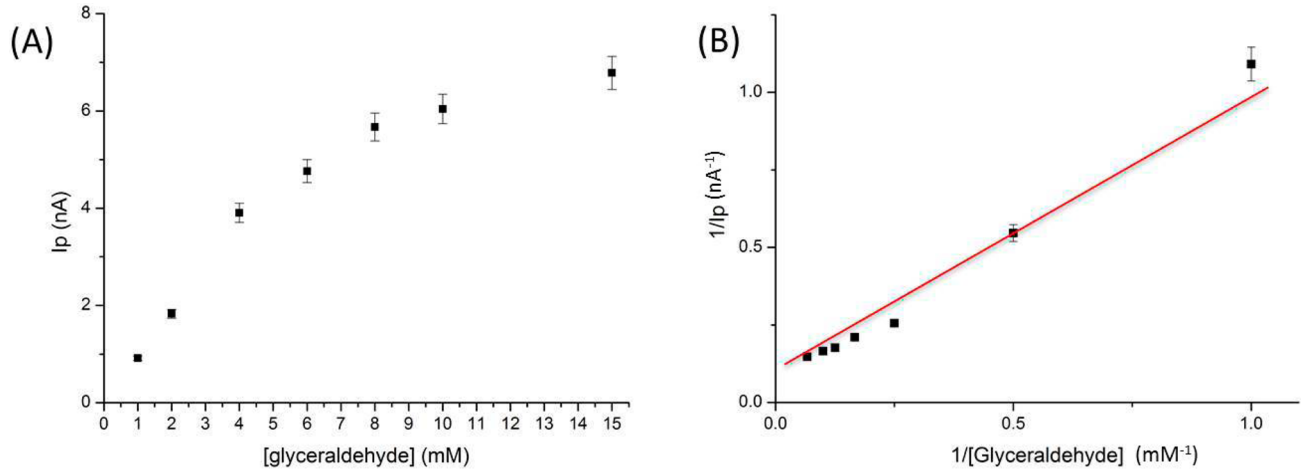

Figure 8. Calibration curve of peak current vs glyceraldehyde concentration (A) and Lineweaver–Burk plot (B) of His-IIN-modified gold electrodes.

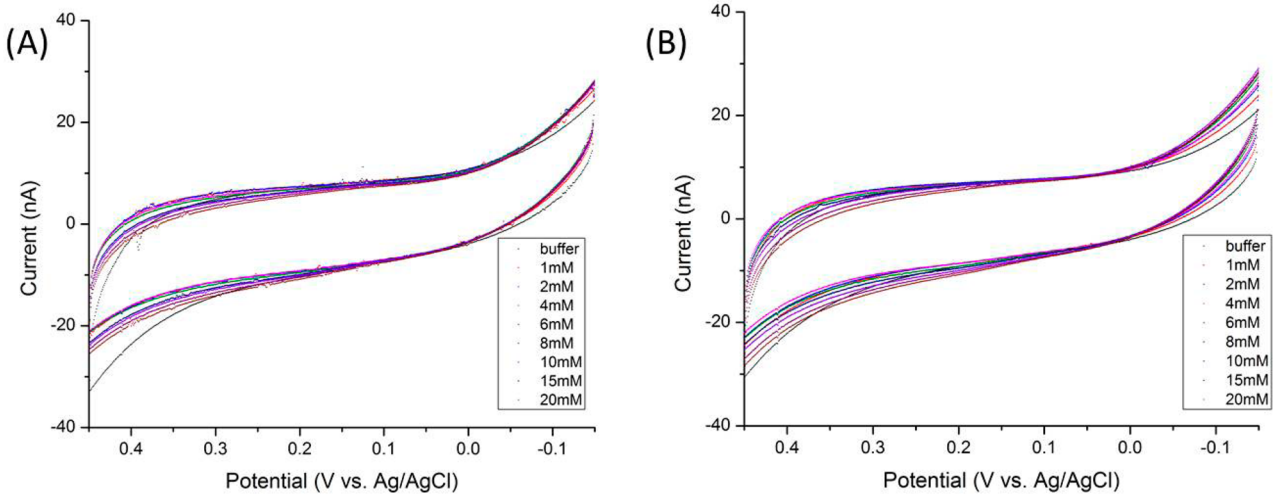

Figure 9. Cyclic voltammograms of (A) His-IIIC- and (B) His-IIIN-modified gold electrodes in 50 mM phosphate buffer (pH 7.4) with 0.1 M KNO_3 as the supporting electrolyte at a scan rate of 5 mV/s. Concentrations correspond to increasing concentrations of glyceraldehyde.

Michaelis–Menten kinetics, and a Lineweaver–Burk plot gives a K_m of 3.89 ± 0.52 mM and a V_{max} of 1.19 ± 0.16 nA; the reported wild-type PQQ-AlDH K_m is 12 mM.[24] The results show that the His-IC orientation is capable of DET; however, the electron transfer rate is slow. This can be explained as the substrate accessibility to the enzyme active site being inhibited with this orientation arrangement and the distance between the single heme *c* group and the gold surface being too long for efficient electron tunneling. His-IN showed no ability to directly transfer electrons, which is in accordance with the previous low-immobilized enzyme activity assays, combined with the fact that this orientation is unfavorable for efficient DET, because the PQQ active site is in this general area of subunit I.

Cyclic voltammograms of His-IIC and His-IIN are shown in Figure 7. Subunit II is the subunit with multiple heme *c* groups. In those two orientations, enzymes are tethered to the electrode surfaces by connecting subunit II to the Ni-NTA linker, so electron transfer can occur through the PQQ cofactor to multiple heme *c* groups and to the electrode surface via the closest heme *c* group. Cyclic voltammograms of His-IIN show a catalytic peak at 229 mV versus Ag|AgCl, which exhibits direct electron transfer, while His-IIC shows no peak in this scan range, which is expected because the immobilized enzyme assays showed no significant protein was bound to the gold electrodes. A calibration curve and Lineweaver–Burk plot of the electrochemical assay data for His-IIN-modified gold electrodes are shown in Figure 8. The calibration curve of His-IIN-modified gold electrodes also follows Michaelis–Menten kinetics, and a Lineweaver–Burk plot gives a K_m of 5.07 ± 0.49 mM and a V_{max} of 7.94 ± 0.63 nA. His-IIN-modified gold electrodes show a 6-fold DET rate increase over that of His-IC-modified gold electrodes. This is expected, because the multiple-heme *c* subunit is attached to the electrode surface allowing for facile electron transfer yet the PQQ subunit (subunit I) is still exposed to the substrate.

Cyclic voltammograms of His-IIIC- and His-IIIN-modified gold electrodes are shown in Figure 9. Subunit III is the peptide subunit that has no known, nonstructural function. With this subunit attached to electrode surface, no heme *c* group or PQQ cofactor is in the proximity of the electrode surface, so the cyclic voltammograms showed no peak structure and no direct electron transfer.

Lastly, for the purpose of direct comparison, His-IC-, His-IIN-, and His-IIIN-modified gold electrodes are chosen to represent different enzyme orientations toward the electrode. The His-IIIN electrode showed no catalytic peak in the scan range. This result is in accordance with our prediction; with the

dx.doi.org/10.1021/cs400316b | *ACS Catal.* 2013, 3, 1756–1763

peptide subunit anchored on the modified surface, the heme-containing subunits are stretched away from the electrode surface, resulting in a long heme−electrode distance that prevents electron transfer from occurring. The His-IC electrode showed a small oxidation peak (1.01 ± 0.11 nA) at 203 ± 9 mV versus Ag|AgCl and a clearer reduction peak at 123 ± 6 mV versus Ag|AgCl. Compared to the oxidation potential of the His-IIN electrode (229 ± 4 mV vs Ag|AgCl) and the reduction potential of 98 ± 2 mV versus Ag|AgCl, the oxidation potential shifted by 26 mV and the reduction potential by 25 mV, which can be caused by different internal electron transfer pathways. The His-IIN-modified gold electrode showed a 6.6-fold catalytic current increase (6.71 ± 0.52 nA vs 1.01 ± 0.11 nA), which indicates this orientation is preferable for fast electron transfer. Our explanation for this result is that His-IIN gives good accessibility of the substrate to the active site of the enzyme and electrons can be quickly transferred via multi-heme *c* groups and released to the electrode surface from the closest heme *c* group. This orientation has a comparatively small tunneling distance. His-IC has its active site buried close to the electrode surface, so it is more difficult for the substrate to diffuse to the active site and the electrons produced at the active site to transfer to the single heme *c* group in subunit I and then transfer to the gold electrode, which is a less optimal pathway.

CONCLUSIONS

In this work, we have addressed the importance of enzyme orientation in efficient direct electron transfer. Control of the orientation has been achieved by specifically binding six PQQ-AlDHs to Ni-NTA-modified gold electrodes via His-tags on different subunits of the enzymes. The ability of DET of each orientation arrangement was measured with cyclic voltammetry. It is demonstrated that only with PQQ-AlDH oriented to expose its active site to the substrate and the good proximity between heme *c* groups and the electrode, efficient DET is observed. Thus, proper orientation is mandatory for efficient direct electron transfer.

ASSOCIATED CONTENT

Supporting Information

Procedures for gel electrophoresis and representative gels as well as control cyclic voltammograms. This material is available free of charge via the Internet at http://pubs.acs.org.

AUTHOR INFORMATION

Corresponding Author

*E-mail: minteer@chem.utah.edu. Phone: (801) 587-8325.

Notes

The authors declare no competing financial interest.

ACKNOWLEDGMENTS

We acknowledge the National Science Foundation (Grant #1159843) and the United Soybean Board for funding.

REFERENCES

(1) Habrioux, A.; Merle, G.; Servat, K.; Kokoh, K. B.; Innocent, C.; Cretin, M.; Tingry, S. *J. Electroanal. Chem.* **2008**, *622* (1), 97−102.
(2) Kerr, J.; Minteer, S. D. *Biomol. Catal.* **2008**, *986*, 334−353.
(3) Arechederra, R. L.; Minteer, S. D. *Fuel Cells* **2009**, *9* (1), 63−69.
(4) (a) Spadiut, O.; Pisanelli, I.; Maischberger, T.; Peterbauer, C.; Gorton, L.; Chaiyen, P.; Haltrich, D. *J. Biotechnol.* **2009**, *139*, 250−257. (b) Arechederra, R. L.; Treu, B. L.; Minteer, S. D. *J. Power Sources* **2007**, *173*, 156−161. (c) Zafar, M. N.; Beden, N.; Leech, D.; Sygmund, C.; Ludwig, R.; Gorton, L. *Anal. Bioanal. Chem.* **2012**, *402* (6), 2069−2077.
(5) (a) Sokic-Lazic, D.; Arechederra, R. L.; Treu, B. L.; Minteer, S. D. *Electroanalysis* **2010**, *22* (7−8), 757−764. (b) Sokic-Lazic, D.; Minteer, S. D. *Biosens. Bioelectron.* **2008**, *24*, 945−950.
(6) (a) Barriere, F.; Kavanaugh, P.; Leech, D.; Laccase-Glucose Oxidase, A. *Electrochim. Acta* **2006**, *51* (24), 5187−5192. (b) Barton, S. C.; Kim, H.; Binyamin, G.; Zhang, Y.; Heller, A. *J. Phys. Chem. B* **2001**, *105* (47), 11917−11921. (c) He, J.-f.; Zhu, Q.-h.; Deng, Q.-y. *Spectrochim. Acta, Part A* **2007**, *67A* (5), 1297−1305. (d) Mano, N.; Mao, F.; Heller, A. *Electroanal. Chem.* **2005**, *574* (2), 347−357. (e) Meredith, M. T.; Glatzhofer, D.; Kao, D.-Y.; Schmidtke, D. W.; Hickey, D. *J. Electrochem. Soc.* **2011**, *158* (2), B166−B174.
(7) (a) Kavanagh, P.; Boland, S.; Jenkins, P.; Leech, D. *Fuel Cells* **2009**, *9* (1), 79−84. (b) Hudak, N. S.; Gallaway, J. W. *J. Electrochem. Soc.* **2009**, *156* (1), B9.
(8) Ghindilis, A. L.; Atanasov, P.; Wilkins, E. *Electroanalysis* **1997**, *9* (9), 661−674.
(9) (a) Tsujimura, S.; Kano, K.; Ikeda, T. *Electrochemistry (Tokyo, Jpn.)* **2002**, *70* (12), 940−942. (b) Mano, N.; Kim, H.; Zhang, Y.; Heller, A. *J. Am. Chem. Soc.* **2002**, *124* (22), 6480−6486.
(10) Coman, V.; Vaz-Dominguez, C.; Ludwig, R.; Herreither, W.; Haltrich, D.; De Lacey, A. L.; Ruzgas, T.; Gorton, L.; Shleev, S. *Phys. Chem. Chem. Phys.* **2008**, *10* (40), 6093−6096.
(11) (a) Laurinavicius, V.; Razumiene, J.; Ramanavicius, A.; Ryabov, A. *Biosens. Bioelectron.* **2004**, *20*, 1217−1222. (b) Treu, B. L.; Minteer, S. D. *Polym. Mater. Sci. Eng.* **2005**, *92*, 192−193. (c) Treu, B. L. Development of a PQQ-dependent ADH Bianode. Ph.D. Thesis, Saint Louis University, St. Louis, 2005. (d) Kamitaka, Y.; Tsujimura, S.; Kano, K. *Chem. Lett.* **2007**, *36* (2), 218−219.
(12) Ikeda, H.; Kobayashi, D.; Matsushita, F.; Sagara, T.; Niki, D. *J. Electroanal. Chem.* **1993**, *361* (1−2), 221−228.
(13) Sugisawa, T.; Hoshino, T. *Biosci., Biotechnol., Biochem.* **2002**, *66*, 57−64.
(14) (a) Treu, B. L.; Arechederra, R.; Minteer, S. D. *J. Nanosci. Nanotechnol.* **2009**, *9* (4), 2374−2380. (b) de Aquino Neto, S.; Suda, E.; Xu, S.; Meredith, M. T.; de Andrade, A. R.; Minteer, S. D. *Electrochim. Acta* **2013**, *87*, 323−329.
(15) Zebda, A.; Gondran, C.; Le Goff, A.; Holzinger, M.; Cinquin, P.; Cosnier, S. *Nat. Commun.* **2011**, *2* (2), 370−371.
(16) Lim, J.; Cirigliano, N.; Wang, J.; Dunn, B. *Phys. Chem. Chem. Phys.* **2007**, *9* (15), 1809−1814.
(17) (a) Willner, I.; Heleg-Shabtai, V.; Blonder, R.; Katz, E.; Tao, G.; Buckmann, A. F.; Heller, A. *J. Am. Chem. Soc.* **1996**, *118* (42), 10321−10322. (b) Zayats, M.; Katz, E.; Baron, R.; Willner, I. *J. Am. Chem. Soc.* **2005**, *127* (35), 12400−12406.
(18) (a) Pardo-Yissar, V.; Katz, E.; Willner, I.; Kotlyar, A. B.; Sanders, C.; Lill, H. *Faraday Discuss.* **2000**, *116*, 119−134. (b) Katz, E. *J. Electroanal. Chem.* **1994**, *365*, 157−164.
(19) (a) Johnson, D.; Martin, L. *J. Am. Chem. Soc.* **2005**, *127* (7), 2018−2019. (b) Holland, J. T.; Lau, C.; Brozik, S.; Atanassov, P.; Banta, S. *J. Am. Chem. Soc.* **2011**, *133* (48), 19262−19265.
(20) Ataka, K.; Giess, F.; Knoll, W.; Naumann, R.; Haber-Pohlmeier, S.; Richter, B.; Heberle, J. *J. Am. Chem. Soc.* **2004**, *126* (49), 16199−16206.
(21) Xu, S.; Minteer, S. *ACS Catal.* **2012**, *2* (1), 91−94.
(22) Haddour, N.; Cosnier, S. *J. Am. Chem. Soc.* **2005**, *127* (16), 5752−5753.
(23) Toyama, H.; Mathews, F. S.; Adachi, O.; Matsushita, K. *Arch. Biochem. Biophys.* **2004**, *428*, 10−21.
(24) Fukaya, M.; Tayama, K.; Okumura, H.; Kawamura, Y.; Beppu, T. *Appl. Microbiol. Biotechnol.* **1989**, *32* (2), 176−180.